Formin INF2 regulates MAL-mediated transport of Lck to the plasma membrane of human T lymphocytes

Laura Andrés-Delgado,[1] Olga M. Antón,[1] Ricardo Madrid,[1] Jennifer A. Byrne,[2] and Miguel A. Alonso[1]

[1]Centro de Biología Molecular Severo Ochoa, CSIC-UAM, Cantoblanco, Madrid, Spain; and [2]Children's Cancer Research Unit and the University of Sydney Department of Pediatrics and Child's Health, The Children's Hospital at Westmead, Westmead, Australia

Expression of the src-family kinase lymphocyte-specific protein tyrosine kinase (Lck) at the plasma membrane is essential for it to fulfill its pivotal role in signal transduction in T lymphocytes. MAL, an integral membrane protein expressed in specific types of lymphoma, has been shown to play an important role in targeting Lck to the plasma membrane. Here we report that MAL interacts with *In*verted *F*ormin2 (INF2), a formin with the atypical property of promoting not only actin polymerization but also its depolymerization. In Jurkat T cells, INF2 colocalizes with MAL at the cell periphery and pericentriolar endosomes and along microtubules. Videomicroscopic analysis revealed that the MAL$^+$ vesicles transporting Lck to the plasma membrane move along microtubule tracks. Knockdown of INF2 greatly reduced the formation of MAL$^+$ transport vesicles and the levels of Lck at the plasma membrane and impaired formation of a normal immunologic synapse. The actin polymerization and depolymerization activities of INF2 were both required for efficient Lck targeting. Cdc42 and Rac1, which bind to INF2, regulate Lck transport in both Jurkat and primary human T cells. Thus, INF2 collaborates with MAL in the formation of specific carriers for targeting Lck to the plasma membrane in a process regulated by Cdc42 and Rac1. (*Blood*. 2010;116(26): 5919-5929)

Introduction

The activation of the src-family kinase lymphocyte-specific protein tyrosine kinase (Lck) is one of the earliest intracellular events downstream T-cell receptor (TCR) recognition. Activated Lck phosphorylates tyrosine residues of CD3, ζ-chain–associated protein kinase 70, and other substrates, initiating various signaling cascades that result in T-cell activation and proliferation.[1,2] Lck is predominantly associated with the cytosolic side of the plasma membrane, a localization that is consistent with its importance in TCR-mediated early signaling events.[3] Transport of Lck to the plasma membrane relies on the exocytic pathway[4] and requires addition of myristate and palmitate to the glycine and the 2 cysteine residues of its N-terminal Gly-Cys-Val-Cys sequence.[5,6] Palmitoylation/depalmitoylation of Lck can also contribute to exchange Lck between the plasma membrane and the cytosol.[7] Lck acylation is also essential for activation of downstream signaling pathways[6] and partitioning into detergent-resistant membranes[5] that are postulated to contain specialized membrane microdomains.[8] MAL is an integral membrane protein exclusively detected in detergent-resistant membranes of epithelial cells and human T lymphocytes.[9,10] Recent work established that MAL, which was originally characterized as a component of the machinery for specialized transport from the Golgi to the apical surface of polarized epithelial cells,[10-12] mediates a specialized route responsible for Lck transport to the plasma membrane of human T cells.[13] The questions remain as to what other machinery collaborates with MAL to transport Lck and how this process is regulated.

The important role of MAL in intracellular protein transport implies that alterations in MAL expression or subcellular distribution could be reflected in abnormal functioning of the cells. It has been reported that MAL is overexpressed in cutaneous T-cell lymphoma resistant to α-interferon therapy.[14] Although MAL expression is normally absent from normal B lymphocytes, MAL expression has been found in primary mediastinal B-cell lymphoma[15,16] and in a subset of Hodgkin lymphoma with an adverse outcome.[17,18] Therefore, in addition to the interest of the elucidation of the mechanism of MAL-mediated transport of Lck in normal T cells, the understanding of MAL function in normal cells would be of great help to unveil its role in tumor cells.

The mechanism and regulation of MAL-mediated Lck transport in T lymphocytes are addressed in the present paper through the identification of human *In*verted *F*ormin2 (INF2) as a binding partner of MAL. INF2 domain organization is similar to that of the diaphanous-related group of formins (Drfs), which are direct effectors of Rho-family guanosine triphosphate (GTP)ases. Drfs mediate actin filament formation,[19,20] coordination of microtubules and the actin cytoskeleton,[21] and microtubule stabilization.[22] Drfs have an autoregulatory domain at their carboxyl terminus, known as the diaphanous autoregulatory domain (DAD), which is separated by formin homology (FH) domains 1-2 from an amino-terminal diaphanous inhibitory domain (DID). The DAD interacts with the DID to close the Drf molecule and maintain it in an inactive state. The binding of the effector Rho GTPase in its GTP-loaded form to the DID allows the generation of linear actin filaments by releasing the Drf from auto-inhibition.[23] Remarkably, unlike other formins, INF2 has the unusual ability to accelerate not only actin polymerization but also its depolymerization.[24] Herein, we report that INF2 colocalizes and interacts with MAL and that INF2 is necessary

Submitted August 4, 2010; accepted September 21, 2010. Prepublished online as *Blood* First Edition paper, September 29, 2010; DOI 10.1182/blood-2010-08-300665.

The online version of this article contains a data supplement.

The publication costs of this article were defrayed in part by page charge payment. Therefore, and solely to indicate this fact, this article is hereby marked "advertisement" in accordance with 18 USC section 1734.

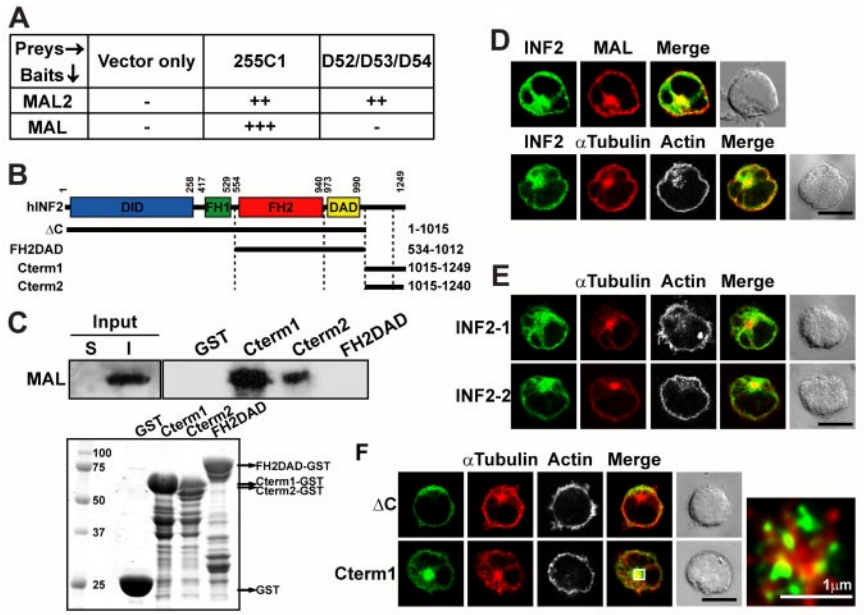

Figure 1. Characterization of INF2 as a MAL-interacting protein and analysis of its subcellular distribution in Jurkat cells. (A) Yeast HF7C strain cells were cotransformed with the pAD-GAL4 255C1 cDNA obtained in the yeast 2-hybrid screen and bait constructs encoding either full-length MAL or MAL2 or the indicated D52-like prey proteins as negative controls. Yeast growth on solid media at 30°C was evaluated as follows: –, no growth after 6-8 days; ++, growth after 3-4 days; +++, growth after 1-2 days. Identical results were obtained for all 3 D52-like proteins. (B) Schematic of the INF2-1 proteins expressed in the experiments in this Figure. (C) The 1% Triton-X-100 insoluble (I) membrane fraction of Jurkat cells was separated from the soluble fraction (S) and, after solublization with 60mM octyl-glucoside, was subjected to pull-down analysis with GST alone or fused to the indicated INF2 fragments. The presence of endogenous MAL was determined by immunoblotting with mAb 6D9 (top). The Coomassie blue staining of the GST proteins used is shown (bottom). (D) Jurkat cells transiently transfected (top) or not (bottom) with Cherry-MAL were stained for endogenous INF2 using anti-INF2 antibodies and secondary antibodies coupled to Alexa-488 (top) or for INF2, α-tubulin, and F-actin using antibodies to INF2 and α-tubulin and secondary antibodies coupled to Alexa-488 or Alexa-647 and with TRITC-phalloidin, respectively (bottom). (E) Jurkat cells transiently expressing GFP fused to INF2-1 or INF2-2 were fixed and stained for α-tubulin and F-actin with anti–α-tubulin antibodies followed by secondary antibodies coupled to Alexa-647 and with TRITC-phalloidin, respectively. (F) Jurkat cells transiently expressing GFP fusions of the indicated fragments of INF2-1 were used to analyze the distribution of α-tubulin and F-actin with anti–α-tubulin antibodies followed by secondary antibodies coupled to Alexa-647 and TRITC-phalloidin, respectively. A representative x/y plane is shown in each case. A deconvoluted enlargement of the pericentriolar region (boxed region) is included in the case of Cterm1-transfected cells to show that Cterm1 surrounds the microtubule-organizing center. A pile-up of 2 medial confocal stacks is presented in D-E. The staining of F-actin is presented in gray in D-F to help its visualization. A Nomarsky image of the cell field is included in all the cases. Scale bars correspond to 5 μm unless other value is indicated.

for normal subcellular distribution of Lck and correct formation of immunologic synapse. Furthermore, INF2 is essential for formation of the MAL$^+$ vesicular carriers that transport Lck to the plasma membrane of T lymphocytes. The MAL$^+$ vesicular carriers transporting Lck move along microtubule tracks in a process that is dependent on the actin polymerization and depolymerization activities of INF2. We have also found that Lck targeting is regulated by the Rho-family GTPases Cdc42 and Rac1, which bind the DID of INF2. Our results reveal a pathway whereby Rac1, Cdc42, INF2, and MAL regulate the targeting of Lck to the plasma membrane of T lymphocytes.

Methods

Reagents and antibodies

The mouse monoclonal antibody (mAb) 6D9 to human MAL[9] and the rabbit polyclonal antibodies to INF2[25] have been described previously. The mouse mAb DM1A to α-tubulin was purchased from Sigma-Aldrich; the mAb and the rabbit polyclonal antibodies to Lck were from BD Biosciences. The mAb to CD3 and that to murine CD4 were kindly provided by Dr Alarcón (Centro de Biología Molecular Severo Ochoa) and Dr Rojo (Centro de Investigaciones Biológicas, Madrid, Spain), respectively. The antibodies to RhoA, Rac1, and Cdc42 were from BD Biosciences. The anti–glyceraldehyde 3-phosphate dehydrogenase (GADPH) antibody was from Santa Cruz Biotechnology. Fluorescent secondary anti–rabbit or anti–mouse immunoglobulin G antibodies and tetramethylrhodamine isothiocyanate (TRITC)–phalloidin were obtained from Molecular Probes (Invitrogen). Secondary anti–rabbit or anti–mouse immunoglobulin G antibodies coupled to horseradish peroxidase were from Jackson ImmunoResearch Laboratories.

Cell-culture conditions

Human T lymphoblastoid Jurkat cells were grown in RPMI 1640 supplemented with 10% fetal bovine serum (Sigma-Aldrich), 50 U/mL penicillin, and 50 μg/mL streptomycin at 37°C in an atmosphere of 5% CO_2/95% air. For formation of T-cell–antigen-presenting cell conjugates, Raji B cells (3.0×10^6 cells/mL) were incubated for 20 minutes in the presence or absence of 4 μg/mL staphylococcal enterotoxin E superantigen (Toxin Technology) and mixed with an equal number of Jurkat cells (5.0×10^5 cells/well) in a final volume of 50 μL, incubated at 37°C for 15 minutes and plated onto poly(L)lysine-coated slides. For experiments with human primary T cells, freshly isolated T lymphocytes from healthy donors were used following the guidelines of the Bioethics Committee of the Spanish Research Council and with the approval of the institutional management committee of the Centro de Biología Molecular "Severo Ochoa" (Madrid, Spain).

Analysis of direct interactions by the yeast 2-hybrid system

Paired baits (pAS2-1 constructs) and preys (pACT2 or pAD-GAL4 constructs) were transfected into Hf7c cells, as described elsewhere,[26] and their interactions assessed by qualitatively determining *His3* reporter gene activity.[27] All constructs used were verified by DNA sequencing. Control prey constructs encoding D52-like fusion proteins have been described elsewhere.[28]

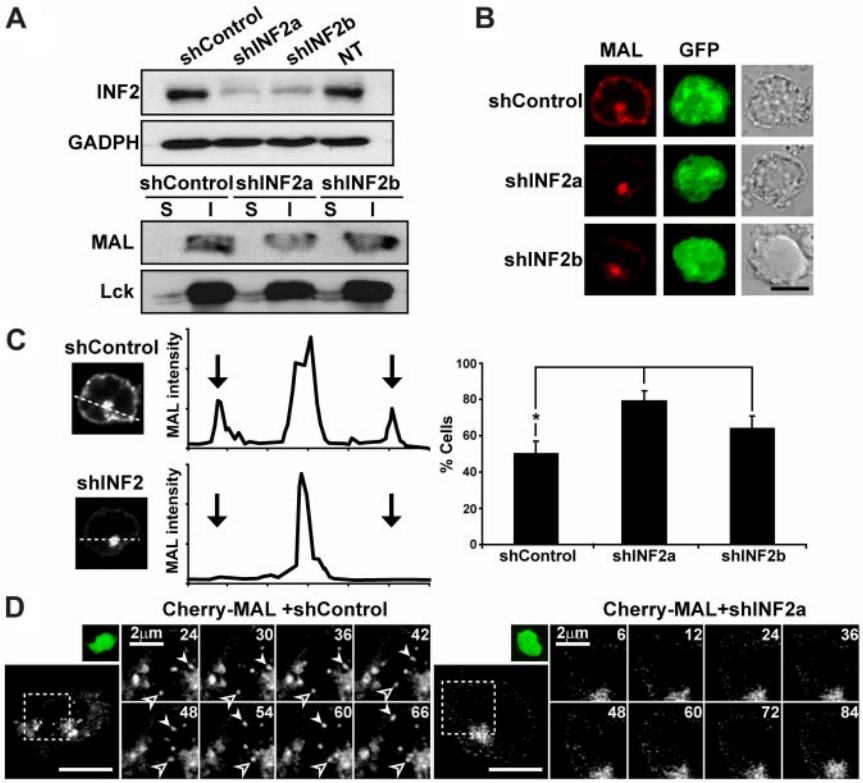

Figure 2. INF2 knockdown blocks the exit of MAL vesicles from perinuclear endosomes and decreases the expression of MAL at the plasma membrane. (A-C) Wild-type Jurkat cells (A) or Jurkat cell transiently expressing Cherry-MAL (B-C) were transfected or not (NT) with a DNA construct coexpressing GFP and shControl, or shINF2a or shINF2b, which are targeted to the coding or 3′ untranslated regions, respectively, of INF2 mRNA. Cells were processed for immunoblotting with anti-INF2 antibodies to examine the levels of INF2 or with anti-GADPH antibodies as a loading control (A, top). The 1% Triton-X-100 insoluble (I) membrane fraction of Jurkat cells was separated from the soluble fraction (S), and equivalent aliquots were immunoblotted for MAL and Lck (A bottom). Cells were also processed for fluorescence microscopy to analyze the distribution of MAL (B-C). The intensity of MAL staining in Jurkat cells was measured by densitometric analysis along rectilinear lines as that shown in a representative experiment (C, left). Arrows indicate the position of the periphery of the cell (C middle). The histogram shows the mean percentage ± SEM of cells with low levels of MAL at the plasma membrane as measured as described in "Methods" (C right). Staining intensity was measured in > 50 cells per experiment. Three independent experiments were performed (*$P < .05$). (D) Jurkat cells transiently expressing Cherry-MAL were transfected with a plasmid coexpressing GFP and shControl or shINF2a for 48 hours, the activity being captured with time-lapse videomicroscopy. Transfected cells were identified by expression of GFP (small top panel). The processes occurring in the cell (large bottom panel) within the boxed region are shown at higher magnification in the right panels. Solid and empty arrowheads indicate 2 vesicles transporting MAL from the pericentriolar region to the plasma membrane or from the plasma membrane to the pericentriolar region, respectively. Numbers indicate time in seconds. Scale bars correspond to 5 μm unless other value is indicated.

DNA constructs and transfection conditions

The DNA constructs expressing green fluorescent protein (GFP) or Cherry fusions of wild-type INF2-1, INF2-2,or INF2-1 proteins with point mutations in sequences encoding the FH2 and/or the DAD (INF2-K/A; INF2-3L/A, and INF2-K/A-3L/A mutants) as well as the constructs expressing INF2 fragments or glutathione transferase (GST)-INF2 fusion proteins are described elsewhere.[25] The constructs used for expression of INF2 proteins in Jurkat cells contain only the coding sequence of the INF2 mRNA, and, therefore, their expression products are resistant to knockdown by shINF2b, which targets the 3′ untranslated region. The constructs expressing GFP fusions of INF2ΔC or Cterm1 were obtained by standard procedures. The sequences of all constructs were verified by automated sequencing. The pMAL-shRNA/GFP constructs that coexpress GFP and shRNAs specific to human MAL as well as the constructs expressing the Cherry protein appended to the carboxyl terminus of Lck (Lck-Cherry) or the amino terminus of MAL (Cherry-MAL) have been described previously.[13] The DNA constructs for expression of GFP fused to Rho GTPases or GST fused to the Rho GTPase-binding domain of PAK1 (GST-PBD) or Rhotekin (GST-RBD) and the plasmid expressing EB3-GFP were generous gifts from Dr J. Millán (Centro de Biología Molecular, Madrid, Spain). The plasmid expressing GFP-tubulin was from Clontech and that expressing p75-GFP[29] was a kind gift from Dr Rodriguez-Boulan (Cornell University, New York, NY). The DNA construct expressing the ectodomain and transmembrane region of murine CD4 fused to Lck (CD4/Lck) has been described elsewhere.[30] The sequences 5′ GTACCGCTTCAGCATTGTC 3′ or 5′ CTTGGCCATCACATCAACA 3′, which target the coding or 3′ untranslated region, respectively, of INF2 mRNA, separated by a short spacer (5′-TTCAAGAGA-3′) from their reverse complement was cloned under the control of the H1-RNA promoter in the pSuper-Retro-GFP (Oligoengine) vector to generate the plasmids coexpressing GFP and shRNAa or shRNAb specific to human INF2, respectively. The plasmids coexpressing GFP and shRNA specific to human RhoA, Rac1, and Cdc42 were from SABiosciences. The GFP coding sequence was replaced by that encoding the Cherry protein in the construct expressing shRNA to Cdc42 using standard procedures. Jurkat cells and primary human T cells were transfected by electroporation using the Gene Pulser system (Bio-Rad Laboratories). To evaluate the extent of protein knockdown using the shRNA expressing constructs, GFP-expressing cells were separated in a cell sorter and analyzed by immunoblotting with the appropriate antibodies.

Confocal microscopic analysis

Cells were fixed in 4% paraformaldehyde for 15 minutes, rinsed, and treated with 10mM glycine for 5 minutes to quench the aldehyde groups. The cells were permeabilized or not with 0.1% Triton X-100, rinsed, and incubated with 3% bovine serum albumin in phosphate-buffered saline for 15 minutes. Cells were then incubated for 1 hour with the appropriate primary antibodies, rinsed several times, and incubated for 30 minutes with the appropriate combination of secondary antibodies coupled to Alexa-488,

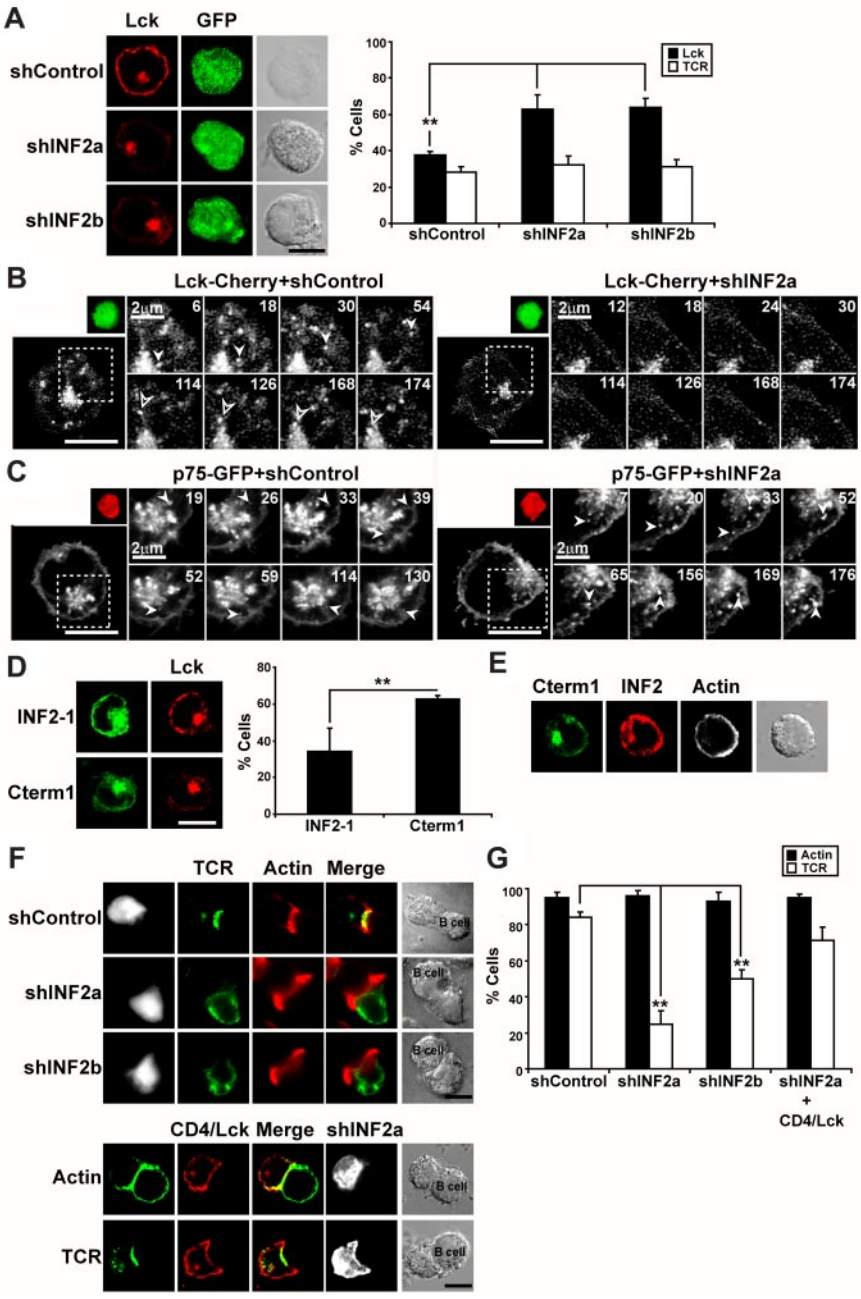

Figure 3. INF2 knockdown blocks the formation of exocytic transport vesicles containing Lck and decreases the expression of Lck at the plasma membrane. (A) The subcellular distribution of endogenous Lck was analyzed in Jurkat cells coexpressing GFP and shControl, shINF2a, or shINF2b using anti-Lck antibodies followed by secondary antibodies coupled to Alexa-647 antibodies. Lck staining intensity was measured by densitometric analysis along rectilinear lines as described for MAL in Figure 2C. The histogram shows the mean percentage ± SEM of cells with low levels of peripheral Lck or TCR/CD3. (B-C) Jurkat cells transiently expressing Lck-Cherry (B) or p75-GFP (C) were cotransfected with a construct coexpressing GFP and shControl or shINF2a (B) or Cherry and shControl or shINF2a (C) for 48 hours, the activity being captured with time-lapse videomicroscopy. Transfected cells were identified by expression of GFP (B) or Cherry (C). The processes occurring in the cell within the boxed regions are shown at higher magnification in the right panels. Arrowheads indicate 2 vesicles transporting Lck to the plasma membrane. Numbers indicate time in seconds. (D) Jurkat cells transiently expressing INF2-1 or Cterm1 were stained for endogenous Lck using anti-Lck antibodies and secondary antibodies coupled to Alexa-647 (left). The histogram shows the mean percentage ± SEM of cells with low levels of peripheral Lck. (E) Jurkat cells transiently expressing GFP fused to Cterm1 were stained for endogenous INF2 using anti-INF2 antibodies and secondary antibodies coupled to Alexa-594 and with TRITC-phalloidin. The staining of F-actin is presented in gray. (F) Jurkat cells coexpressing GFP (top) and the indicated shRNA or a trasmembrane CD4/Lck chimera (bottom) were conjugated to staphylococcal enterotoxin E–pulsed antigen presenting cells (APCs) for 15 minutes. After cell fixation, the distribution of TCR/CD3 and F-actin was analyzed with anti-CD3 antibodies and secondary antibodies coupled to Alexa-647 and with TRITC-phalloidin, respectively. The staining of TCR/CD3 was pseudocolored in green and that of GFP in gray to help visualization of the distribution of TCR/CD3. The cells expressing CD4/Lck were identified with anti–mouse CD4 mAb and secondary antibodies coupled to Alexa-488 (bottom). (G) The histogram represents the mean percentage of transfected Jurkat cells in T-cell–APC conjugates displaying polarized distribution of F-actin or TCR/CD3 to the IS. Three independent experiments were performed in panels A, D, G; $n > 50$ T cells/experiment (**$P < .01$). Scale bars correspond to 5 μm unless other value is indicated.

Alexa-594, or Alexa-647. Actin filaments were detected with TRITC-phalloidin. Coverslips were mounted with Fluoromount (Sigma-Aldrich). Controls to assess labeling specificity included incubations with, or omitting, control primary antibodies. For the quantitative analysis of MAL or Lck distribution, their fluorescence signal was profiled along a line at the equatorial plane of the cell using National Institutes of Health ImageJ Version 1.43m software (http://rsb.info.nih.gov/ij/). The ratio of internal to plasma membrane fluorescence was calculated for each type of Jurkat cell in 3 independent experiments (n = 50 cells for each type of cell). Cells with a ratio greater than 2-fold the mean value of normal Jurkat cells were considered to express low levels of Lck at the plasma membrane. Approximately 48% and 36% of wild-type Jurkat cells met this criterion for MAL and Lck, respectively. Images were obtained by confocal microscopy using an LSM510 META system (Carl Zeiss) coupled to an inverted Axiovert 200 microscope. A 63×/1.4 oil Plan Apochromat objective was used. For time-lapse experiments, cells were maintained at 37°C in Hanks balanced salt solution supplemented with 5% fetal bovine serum. Cell images were captured at 11-second intervals for simultaneous videomicroscopy of Cherry-MAL and GFP-tubulin, every 1.6 seconds in the case of Cherry-MAL and EB3-GFP or every 6 seconds in the case of the individual tracking of Cherry-MAL or Lck-Cherry. Images were analyzed with MetaMorph B.2r6 imaging software (Molecular Devices). Some images were deconvoluted with Huygens 3.0 software (Scientific Volume Imaging). Images were exported in TIFF format, and their brightness and contrast were optimized with Adobe Photoshop.

Pull-down assays

For INF2-MAL pull-down assays, the detergent-insoluble membrane fraction of Jurkat cell was solubilized with 60mM octyl-glucoside and was incubated with 10 μg of GST or GST-INF2 proteins immobilized on GSH-Sepharose beads (GE Healthcare Life Sciences) for 1 hour at 4°C in lysis buffer (10mM MgCl in 25mM Tris-HCl, pH 7.5, 150mM NaCl, 5mM EDTA [ethylenediaminetetraacetic acid], 1% Triton X-100). Beads were washed 3× in lysis buffer, and MAL was detected by immunoblotting with anti-MAL mAb 6D9 using the enhanced chemiluminescence detection kit

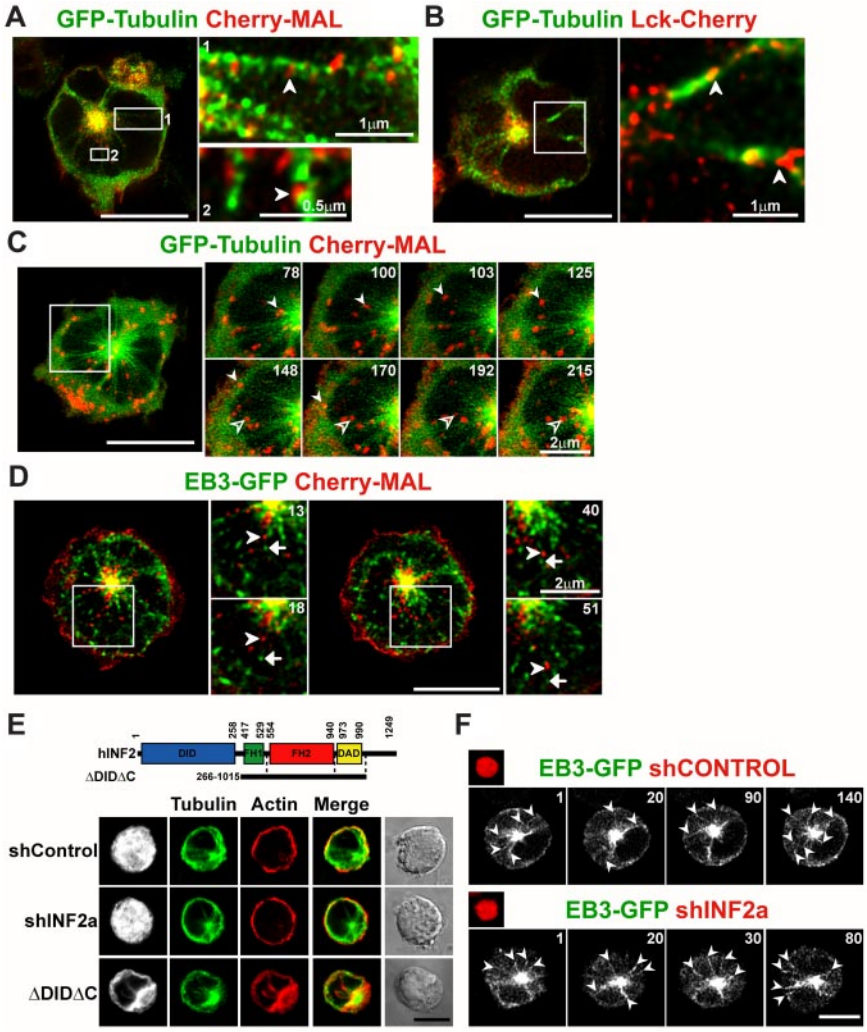

Figure 4. MAL⁺ transport vesicles move along microtubule tracks. (A-B) Jurkat cells coexpressing GFP-tubulin and Cherry-MAL (A) or Lck-Cherry (B) were fixed and analyzed by confocal microscopy. Enlargements of the boxed regions are shown on the right. The arrows indicate MAL⁺ (A) or Lck⁺ (B) vesicles associated with microtubules. (C-D) Jurkat cells were cotransfected with plasmids expressing Cherry-MAL and GFP-tubulin (C) or EB3-GFP (D). After 24 hours, cells were subjected to time-lapse videomicroscopy. The image of a representative cell is shown. Selected frames corresponding to events occurring in the boxed regions during the time-lapse experiment are shown. In panel C, the solid and empty arrowheads indicate 2 MAL⁺ vesicles that move to the plasma membrane or to the pericentrosomal region, respectively, along microtubule tracks. In panel D, the arrowhead indicates a MAL⁺ vesicle moving along a microtubule labeled at its plus tip with EB3, which is indicated by an arrow. Two different areas from the same cell are enlarged in panel D. (E) Jurkat cells coexpressing GFP and shINF2a or transfected with the indicated INF2 construct were fixed, permeabilized, and stained with anti–α-tubulin antibodies followed by Alexa-488 secondary antibodies and with TRITC-phalloidin. The cells expressing the exogenous INF2 fragment were identified with anti-INF2 antibodies and secondary antibodies coupled to Alexa-647 (bottom). The staining of exogenous INF2 is presented in gray. (F) Jurkat cells coexpressing the Cherry protein and the indicated shRNA from the same plasmid were transfected with EB3-GFP and processed for time-lapse videomicroscopy. Arrows indicate microtubules labeled with EB3 at their growing end. Numbers in panels C, D, and F indicate time in seconds. Scale bars correspond to 5 μm unless another value is indicated.

(GE Healthcare Life Sciences). For Rho GTPase pull-down, cells were lysed in 50mM Tris-HCl, pH 7.4, 1mM $MgCl_2$, 2mM EDTA, 300mM NaCl, 0.5% Nonidet P-40, 10% glycerol containing a cocktail of protease inhibitors. Preloading of endogenous Rho GTPases was performed in cell lysates incubated with 50 μM 5′-guanylyl-imidodiphosphate trisodium salt hydrate (GMP-PNP; Roche Applied Science) for 10 minutes at 30°C. The reaction was stopped by adding $MgCl_2$ to a final concentration of 10mM. For binding assays, 10 μg of GST proteins were incubated for 1 hour at 4°C in lysis buffer containing 10mM $MgCl_2$ with the lysates preloaded with GMP-PNP. The beads were washed 3× in interaction buffer, and bound proteins were analyzed by Western blotting with anti-RhoA, -Rac1, or -Cdc42 mAbs.

Statistical analysis

Data are expressed as mean ± SEM. A paired Student *t* test was used to establish the statistical significance of differences between the means.

Results

Identification of human formin INF2 as a MAL-interacting protein

The isoform 1 of formin INF2 (INF2-1) was isolated during a yeast 2-hybrid screen as a binding partner of MAL2,[25] a member of the MAL family of proteins originally identified in a yeast 2-hybrid screen by its interaction with tumor protein D52L2.[27] INF2-1 fragments containing the carboxyl-terminal 255 amino acids, referred to as 255C1, or the entire carboxyl terminal domain (Cterm1), were shown to be sufficient for the interaction with MAL2 in yeast 2-hybrid and pull-down experiments, respectively.[25] Using the same type of assays, we found that the same INF2 fragments also interacts with MAL (Figure 1A-C). As control baits in the yeast 2-hybrid assay, we used distinct D52-like proteins,[28] which interacted specifically with MAL2 but not with MAL (Figure 1A). The equivalent region of the INF2-2 isoform, known as Cterm2, which differs from Cterm1 in the carboxyl-terminal 18-amino acid sequence, also bound MAL whereas the FH2DAD fragment did not (Figure 1C). Immunofluorescence analysis of Jurkat T cells indicated that endogenous INF2 is distributed at the cell periphery, pericentriolar region, and microtubule cytoskeleton (Figure 1D). As expected, given their physical interaction, we found a high level of colocalization between endogenous INF2 and MAL in Jurkat cells (Figure 1D). Expression of exogenous INF2-1 and INF2-2 in Jurkat cells reproduced the distribution of endogenous INF2 (Figure 1E). In keeping with its interaction with MAL, Cterm1 distributed to the cell periphery, although to a lesser extent than did intact INF2-1, and to the pericentriolar region and microtubules as observed for the entire molecule. However, INF2-1 with the Cterm1 deleted (INF2-ΔC) was exclusively targeted to the cell periphery (Figure 1F). Therefore, Cterm1 is responsible

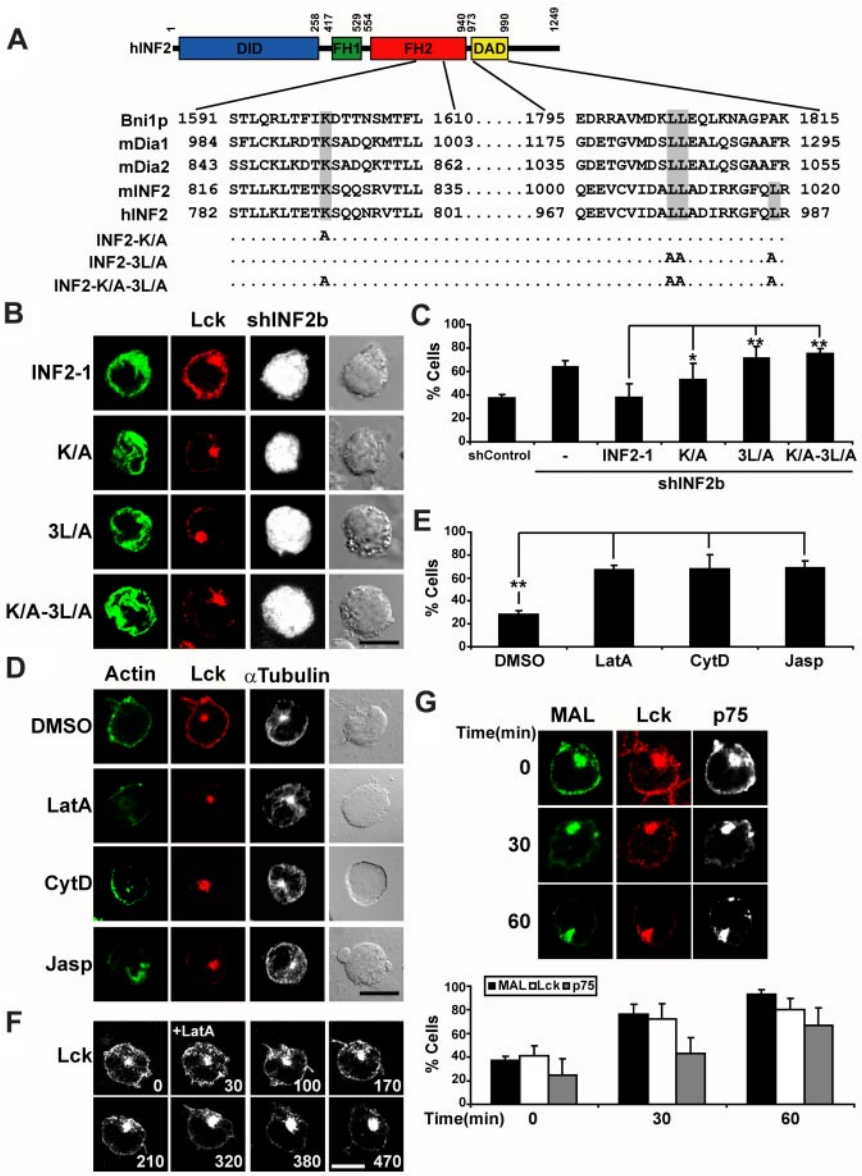

Figure 5. The actin polymerizing and depolymerizing activities of INF2 are both required for efficient targeting of Lck to the plasma membrane. (A) The alignment shows the conservation of Lys[1601] in the FH2 domain of Bnp1 in the corresponding position of mDia1, mDia2, and human and mouse INF2 and the position of the 3 Leu residues critical for F-actin depolymerization in the DAD sequence of mouse and human INF2. Note that the third Leu residue is not present in the Bnp1 or mDia1-2 formins. The residues mutated to alanine in the K/A, 3L/A, and K/A-3L/A INF2-1 mutants are indicated. (B-C) Jurkat cells coexpressing GFP and shControl or shINF2b from the same plasmid were cotransfected with expression plasmids encoding intact Cherry fusions of full-length INF2-1 or INF2-1 proteins with the indicated mutations for 48 hours. The expression of these proteins is resistant to shINF2b as their mRNA lack the INF2 3′ untranslated region to which shINF2b is targeted. Cells were fixed, permeabilized, and subjected to immunofluorescence analysis with anti-Lck antibodies and secondary antibodies coupled to Alexa-647 (Lck; B). The staining of INF2-1 was pseudocolored in green and that of GFP in gray to help visualization of the distribution of INF2-1. The histogram shows the mean percentage ± SEM of cells with low levels of peripheral Lck (C). (D) Jurkat cells were treated with 0.1% dimethyl sulfoxide, 1μM Lantrunculin A (LatA), 2.5μM Cytochalasin D (CytD), or 0.5μM Jasplakinolide (Jasp) for 1 hour. Cells were then fixed and stained for F-actin, Lck, and α-tubulin using TRITC-phalloidin and the appropriate primary antibodies followed by secondary antibodies coupled to Alexa-647 (Lck) or Alexa-488 (α-tubulin). (E) The histogram shows the percentage ± SEM of cells with low levels of peripheral Lck. (F) Jurkat cells expressing Lck-GFP for 24 hours were treated with Lantrunculin (LatA) 30 seconds after start, being subjected to time-lapse videomicroscopy. Numbers indicate time in seconds. (G) Jurkat cells expressing GFP fusions of MAL, Lck, or p75 were incubated for the indicated times in the presence of 100μM nocodazole and analyzed under a confocal microscope. The histogram shows the percentage of cells ± SEM with low levels of peripheral MAL, Lck, or p75. The distribution of p75 is presented in gray. The mean ± SEM of 3 independent experiments is represented in panels C,E,G. Staining intensity in was measured in > 50 cells per experiment; 3 independent experiments were performed (*$P < .05$; **$P < .01$). Scale bars indicate 5 μm.

for the interaction of INF2-1 with MAL and its targeting to the pericentriolar region and microtubules.

INF2 knockdown impairs the formation of transport vesicles containing MAL and produces its intracellular accumulation

To investigate the possible role of INF2 in MAL distribution and function, we used a loss-of-function strategy by using expression of shRNAs (shINF2a and shINF2b) specific to human INF2 mRNA using DNA constructs that simultaneously express GFP to identify the transfected cell population. Expression of shINF2a and shINF2b reduced the levels of endogenous INF2 to 15%-20% of control shRNA (shControl)-transfected cells without affecting the content of MAL or Lck (Figure 2A). Whereas the distribution of MAL was unaffected in shControl-transfected cells, INF2 knockdown greatly reduced the levels of MAL at the cell periphery, pericentriolar region, and radial microtubules, resulting in the intracellular accumulation of MAL (Figure 2B-C). We previously showed that MAL is a dynamic protein that travels in vesicular structures from pericentriolar endosomes to the cell surface for cargo delivery.[13] To examine the requirement of INF2 for the formation of the MAL-positive vesicular carriers, we compared the dynamics of MAL in Jurkat cells with normal or silenced levels of INF2 (Figure 2D and supplemental Video 1, available on the *Blood* Web site; see the Supplemental Materials link at the top of the online article). Whereas MAL-positive vesicles continuously egressed from the pericentriolar region and reached the plasma membranes following linear tracks in control cells, the exit of MAL-positive vesicles was almost completely blocked in INF2-silenced cells. This implies that INF2 expression is necessary for the normal distribution and dynamics of MAL in Jurkat cells.

INF2 is necessary for transport of Lck to the plasma membrane

MAL has been previously shown to be essential for the transport of Lck to the plasma membrane of human T lymphocytes.[13] Because INF2 expression is required for MAL dynamics (Figure 2), we investigated the targeting of Lck to the plasma membrane in INF2-knockdown cells. Consistent with the defect on MAL dynamics, Lck was practically absent at the plasma membrane and accumulated intracellularly in INF2-silenced cells (Figure 3A). The distribution of TCR/CD3, used as a control, was not affected

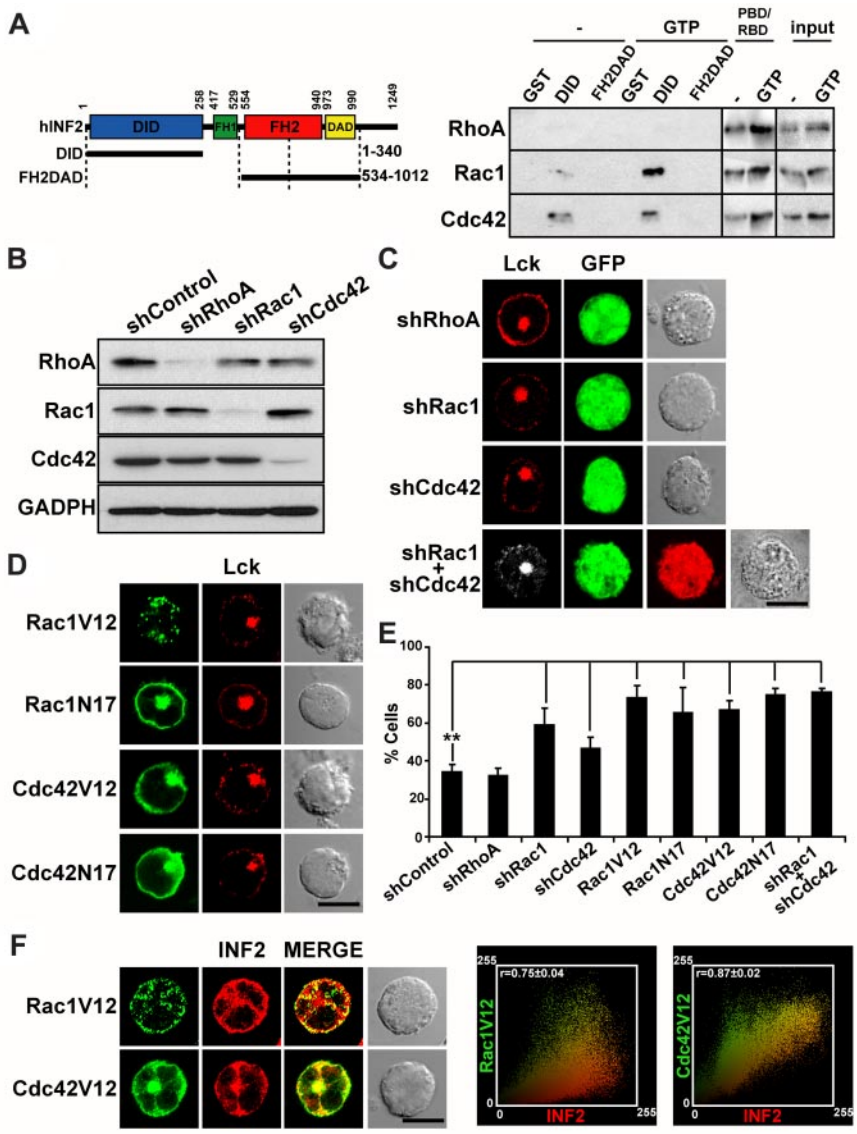

Figure 6. Cdc42 and Rac1 are necessary for targeting Lck to the plasma membrane in Jurkat cells. (A) Jurkat cell extracts were loaded or not with GTP analog GMP-PNP and incubated with GST alone or fused to the indicated fragments of INF2. As controls, the Rho-GTPase binding domains of rhotekin (RBD) or PAK1 (PBD) were used to detect active RhoA or Rac1 and Cdc42, respectively. Ten percent of the original extract was immunoblotted in parallel. (B-C) Jurkat cells expressing GFP and shRNA control or shRNA targeted to RhoA, Cdc42, or Rac1 from the same plasmid were analyzed by immunoblotting with antibodies to the indicated proteins (B). As a loading control, the levels of GADPH were examined. Cells were also fixed, permeabilized, and stained for Lck (C). Double transfectants expressing shRac1 and shCdc42 from plasmids which coexpress GFP and Cherry, respectively, were also analyzed in panel C. (D) Jurkat cells expressing GFP fusions of Rac1V12, Cdc42V12, Rac1N17, or Cdc42N17 for 24 hours were stained for Lck. Anti-Lck antibodies and secondary antibodies coupled to Alexa-647 were used in panels C-D to detect Lck. (E) The percentage of cells with low levels of peripheral Lck in cells with silenced expression or overexpression of the indicated Rho-family GTPases was quantified and summarized as means ± SEM from 3 independent experiments. More than 50 transfected cells were scored in each experiment (**$P < .01$). (F) Jurkat cells transfected with GFP fusions of Rac1V14 or Cdc42V14 for 24 hours were stained for endogenous INF2 using anti-INF2 antibodies and secondary antibodies coupled to Alexa-594. The images shown were deconvoluted. The right panels show plots of colocalization of Rac1V14 or Cdc42V14 with INF2. The Pearson correlation coefficient (r) was 0.75 and 0.87 for Rac1V14/INF2 and Cdc42V14/INF2, respectively. Four independent experiments were performed. Scale bars indicate 5 μm.

by INF2 silencing (Figure 3A). Furthermore, when we compared the dynamics of Lck in Jurkat cells with either normal or silenced levels of INF2, we observed that formation of the exocytic vesicles transporting Lck to the plasma membrane was almost completely impaired in INF2-silenced cells (Figure 3B and supplemental Video 2), whereas transport of the transmembrane protein p75 occurred normally (Figure 3C). Consistent with the interaction of MAL with the Cterm1 domain, overexpression of Cterm1 in Jurkat cells considerably increased the percentage of cells with low expression of Lck at the plasma membrane (Figure 3D). We did not detect any change in the overall distribution of endogenous INF2 in cells overexpressing Cterm1 (Figure 3E), indicating that probably only a small subpool of INF2 collaborates with MAL-mediating Lck transport. Similar to MAL-deficient Jurkat cells,[13] which also express low levels of Lck at the plasma membrane, the translocation of the TCR to the immunologic synapse in T cells with silenced levels of INF2 cells was impaired whereas F-actin polarized normally (Figure 3F-G). The failure of immunologic synapse formation was mostly due to the reduced presence of Lck at the plasma membrane, since forced expression of Lck at the plasma membrane using a transmembrane CD4/Lck chimera restored TCR targeting to the immunologic synapse (Figure 3F-G).

MAL was detected along microtubule arrays radiating from the centrosomal region in Jurkat cells at steady state (Figure 1D). To investigate the possible involvement of microtubules in MAL and Lck trafficking, Jurkat cells were cotransfected with plasmids expressing GFP-tubulin, and Cherry-MAL or Lck-Cherry and were examined by confocal microscopy in unpermeabilized cells to preserve better the distribution of these proteins that, otherwise, might be altered by the detergent permeabilization procedure. MAL was found to distribute in discrete vesicular structures along microtubules (Figure 4A). Transport vesicles containing Lck were found to be associated along microtubules as well (Figure 4B). Moreover, we observed by time-lapse videomicroscopy a continuous exit of MAL-positive vesicles that used microtubule tracks during their movement from the pericentriolar region toward the plasma membrane (Figure 4C). Retrograde trafficking of MAL$^+$ vesicles from the plasma membrane to the pericentriolar region was also observed. Apparently, the anterograde movement of MAL took place along microtubule growing toward the plasma membrane. To

investigate this point further, we monitored simultaneously the movement of Cherry-MAL and GFP-EB3, a protein associated with the plus-growing tip of elongating microtubules.[31] We found that MAL$^+$ vesicles moved along the tracks delineated by EB3 but were not associated with the microtubule tip since MAL moved behind EB3 (Figure 4D). INF2 silencing affected neither the steady state distribution of microtubules and filamentous actin (Figure 4E) nor microtubule dynamics (Figure 4F). Consistent with the effect of other Drfs,[21] the overexpression of a constitutive active mutant of INF2 produced alignment of actin filaments and microtubules (Figure 4E). The results in Figure 4, therefore, indicate that the MAL$^+$ vesicular carriers move to the plasma membrane following tracks of newly formed microtubules in a process probably coordinated by INF2.

Lck transport requires both the actin polymerization and depolymerization activities of INF2

Actin assembly has been shown to power the movement of intracellular vesicles and even intracellular pathogens.[32,33] Mutation of Lys[1601] in the FH2 domain of the yeast Drf Bni1p[34] or in the equivalent position of mDia2[22] impairs the actin nucleation activity of these formins. On the other hand, mutation of 3 critical leucine residues in the DAD of mouse INF2 abrogates its in vitro depolymerization activity.[24] We introduced the same mutations at the equivalent position of human INF2 to generate the K/A, 3L/A, and K/A-3L/A INF2 mutants (Figure 5A) with altered actin polymerization and/or depolymerization activities and used them to determine whether they are able to replace the function of endogenous INF2 in Lck transport. To this end, the transcripts encoding the exogenous INF2 proteins were designed to resist shINF2b expression. In contrast to the expression of intact INF2-1, none of the INF2 mutants was able to restore Lck transport when expressed (Figure 5B-C). The failure of these mutants to substitute endogenous INF2 indicates that both actin polymerization and depolymerization activities of INF2 are required for efficient targeting Lck to the plasma membrane. Consistent with the observed requirement of actin dynamics for Lck transport, treatment of Jurkat cells with different inhibitors that produce depolymerization (Latrunculin A and Cytochalasin D) or stabilization (Jasplakinolide) of actin filaments reduced the Lck levels at the plasma membrane and accumulated the protein in the pericentriolar region (Figure 5D-E). The loss of Lck from the plasma membrane after inhibition of actin polymerization with Lantrunculin A was concomitant with a block in the exit of Lck vesicular carriers from pericentriolar endosomes and the accumulation of Lck at this location (Figure 5F), instead of it being distributed throughout the cytosol as would have been expected if Lantrunculin A simply dissociated Lck from the plasma membrane. Consistent with the results shown in Figure 4, microtubule integrity was required for the targeting of MAL, Lck, and, in agreement with previous observation in other cell types,[29,35] p75 to the plasma membrane as observed in cells treated with the microtubule-disrupting drug nocodazole (Figure 5G).

Cdc42 and Rac1 regulate Lck transport to the plasma membrane

To investigate the binding of Rho-family GTPases to the DID of INF2, we performed pull-down assays using lysates of Jurkat cells in which endogenous Rho GTPases were enriched or not in their GTP-loaded form (Figure 6A). Both Rac1 and Cdc42 bound to the DID fragment under both conditions although to a larger extent in

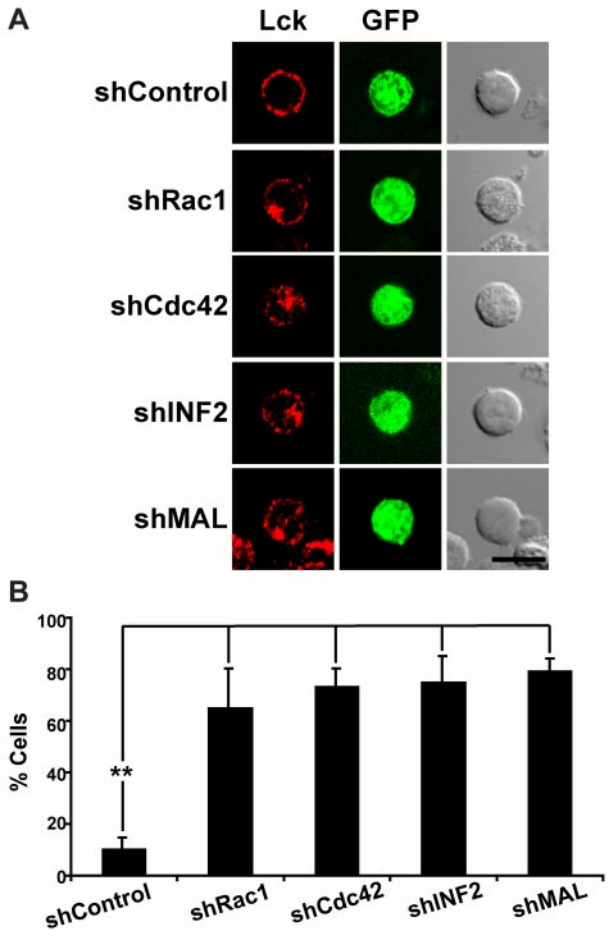

Figure 7. Cdc42, Rac1 and INF2 are necessary for targeting of Lck to the plasma membrane in human primary T cells. (A) Human primary T cells expressing GFP and shControl or shRNA targeted to Rac1, Cdc42, INF2, or MAL from the same plasmid were fixed, permeabilized, and stained for Lck using anti-Lck antibodies and secondary antibodies coupled to Alexa-647. Note that Lck is almost exclusively detected at the plasma membrane in control primary T cells. (B) The histogram represents the mean percentage ± SEM of cells with an intracellular accumulation of Lck. Three independent experiments were performed; > 50 transfected cells were scored in each experiment (**$P < .01$). Scale bar indicates 5 μm.

their GTP-loaded form. No binding of RhoA was observed in either case. Similar results were obtained using lysates of hepatoma $HepG_2$ cells.[25] To investigate whether any of these Rho-family GTPases regulate Lck transport to the plasma membrane, we carried out knockdown experiments using specific shRNA (Figure 6B). The silencing of Cdc42 and Rac1, but not that of RhoA, recapitulated the effect of INF2 (Figure 3) or MAL silencing[13] on the targeting of Lck to the plasma membrane (Figure 6C,E). It is worth noting that the double knockdown of Cdc42 and Rac1 increased the percentage of cells with low levels of Lck at the plasma membrane compared with the single knockdowns (Figure 6C,E), suggesting that Rac1 and Cdc42 function at different moments during Lck transport. To investigate further the role of Rac1 and Cdc42 in this process, we examined the effect of the expression of constitutive active (Rac1V14 and Cdc42V14) or dominant negative (Rac1N17 and Cdc42N17) forms of these 2 Rho GTPases. It is of particular note that in all the cases the cells presented a predominant intracellular accumulation of Lck and very low levels of expression at the plasma membrane (Figure 6D-E). In agreement with a role of Rac1 and Cdc42 on INF2 regulation, we found that these 2 Rho-family GTPases colocalize

partially with INF2 (Figure 6F). In conclusion, both Cdc42 and Rac1 and their GTPase hydrolysis activity are required for exocytic transport of Lck to the plasma membrane.

It is apparent that the effect of INF2, Cdc42, and Rac1 knockdown on Lck targeting to the plasma membrane was not restricted to Jurkat cells as similar experiments in primary T lymphocytes also resulted in diminished expression of Lck at the cell periphery and to its intracellular accumulation (Figure 7). Thus, Lck transport was strictly dependent on Cdc42, Rac1, INF2, and MAL expression in Jurkat cells and primary T lymphocytes.

Discussion

Lck expression at the plasma membrane is critical for its signaling function in T lymphocytes.[6] It is established that Lck relies on the exocytic pathway for targeting to the cell surface.[4] In Jurkat cells, MAL colocalizes extensively with Lck in pericentriolar endosomes and exit together from this location in the same transport vesicles destined for the plasma membrane. Because the formation of the vesicles transporting Lck is severely impaired in cells with silenced MAL expression, MAL was proposed to be an element of the machinery for transporting Lck to the T cell plasma membrane.[13] Despite its crucial role, it is obvious that Lck targeting should involve other molecules that collaborate with MAL in this task. The INF2 formin has recently been implicated in the formation of transcytotic MAL2$^+$ vesicles that transport cargo from the basolateral to the apical surface of epithelial cells.[25] In the present study, we show that INF2 interacts with MAL and mediates the formation of MAL$^+$ vesicular carriers that transport Lck to the plasma membrane of T cells. This mechanism is compatible with exchange mechanisms between the plasma membrane and the cytosol based on palmitoylation/depalmitoylation of Lck.[7] The interaction with MAL involved the carboxyl-terminal Cterm domain of INF2-1, which is not conserved in other formins. The overexpression of this fragment reduced the expression of Lck at the plasma membrane, probably by competing with endogenous INF2 to bind to MAL. Moreover, INF2 knockdown blocked the formation of transport carriers for Lck, caused the intracellular accumulation of Lck, and impaired the formation of a normal immunologic synapse, evoking the effect of MAL silencing.[13] Moreover, knockdown of either Rac1 or Cdc42, which bind INF2, produced the intracellular accumulation of Lck in both Jurkat cells and primary T cells. Therefore, ours results are consistent with a model by which Rac1 and Cdc42 control Lck targeting to the plasma membrane by regulating MAL dynamics through INF2.

Formin mDia1 is induced during T-cell activation and regulates actin polymerization and cell migration.[36] Consistently, T cells from mDia1 knockout mice are defective in migration and proliferation in response to chemotactic or proliferative stimuli, respectively.[37,38] In other cell types, formins mDia1-3 modulate endosome movement through cycles of assembly and disassembly of actin filaments.[39-41] Formins mDia1-3 are responsible for F-actin assembly, but disassembly requires the participation of additional proteins with severing and depolymerizing activities. A distinctive feature of INF2, compared with the mDia1-3 Drfs, is its in vitro capacity both to nucleate and depolymerize actin filaments.[24] Therefore, unlike other formins that only polymerize actin, INF2 can do the entire job of actin polymerization-depolymerization that is required for the formation/movement of vesicular transport carriers. Indeed, our results show that the polymerization and depolymerization activities of INF2 are both required for Lck targeting to the plasma membrane of T cells, suggesting that Lck transport requires actin dynamics. This requirement is consistent with our observation that treatment of Jurkat cells with either Latrunculin A, which binds to actin monomer, Jasplakinolide, which stabilizes actin filaments, or Cytochalasin D, which binds and caps the barbed (fast-growing) end of actin filaments, interfered with the targeting of Lck to the plasma membrane. In cells with actin polymerization inhibited by Lantruculin A, there was a block in the exit of transport vesicles with Lck from pericentriolar endosomes paralleled by an increased presence of Lck at those endosomes instead of it being distributed throughout the cytosol as would have been expected if the inhibition of actin polymerization simply dissociated Lck from the plasma membrane. The possibility remains that the dissociated Lck molecules associate very rapidly to internal membranes. It is of particular note that the movement of the MAL$^+$ vesicular carriers that transport Lck takes place along microtubules and requires microtubule integrity. This observation is consistent with the alignment of actin filaments and microtubules induced by constitutively active INF2. Src transport to the plasma membrane is regulated by RhoB and mDia1 and requires actin polymerization but not microtubule integrity.[42,43] Therefore, although the processes of Src and Lck transport are regulated by Rho-family GTPases and formin proteins, their mechanisms appear to be different.

The DID of the INF2 molecule interacts with Cdc42 and Rac1 but not with RhoA. In agreement with the lack of binding of RhoA, INF2 lacks an N-terminal extension to the DID like that present in the Rho-regulated formins mDia1-2, and that in mDia1 was found to form part of the RhoC binding site.[44] Consistent with the interaction of INF2 with Cdc42 and Rac1, we have found that the 2 Rho-family GTPases are necessary for the efficient transport of Lck to the plasma membrane and appear to function at different steps in the Lck transport process. Remarkably, the expression of constitutive-active or dominant-negative forms of either of these Rho-family GTPases induced the intracellular accumulation of Lck, mimicking the effect of their individual silencing. This result indicates that Lck transport requires dynamic Rac1 and Cdc42 cycling between their GTP- and guanosine diphosphate-loaded states as proposed for RhoB for mDia2-mediated endosome movement.[39] Similar, one possible explanation for our findings is that INF2 needs to be, in turn, dynamically regulated by Rac1 and Cdc42 for Lck transport, what is consistent with our finding showing the requirement of actin dynamics for this process.

Silencing of either MAL or INF2 produced the intracellular accumulation of Lck in pericentriolar endosomes. A similar effect on Lck distribution has recently been reported in Jurkat cells knocked down for Uncoordinated 119 protein (Unc119) or Rab11.[45] This study showed that Unc119 binds to Rab11 and activates its GTPase activity, which, in turn, modulates the binding of myosin 5B, a key Rab11 effector with the ability to move along actin filaments and drive endosome movement.[46] It is also worth noting that HIV infection reduces the expression of Lck at the plasma membrane by causing the intracellular retention of the molecule by a Nef expression–dependent mechanism.[47] Moreover, the individual expression of Nef recapitulates the effect of HIV infection on Lck distribution.[48] Therefore, there is a remarkable similarity in the overall effect on Lck distribution of Nef expression and that of INF2, MAL, Unc119, or Rab11 silencing. The functional integration of all these proteins in a single pathway for Lck transport would be a major achievement.

Although expression of Lck at the plasma membrane is essential for T-cell function,[6] little was known about the mechanism of Lck targeting. Although other mechanisms might also coexist,[7] our findings in Jurkat cells and primary human T lymphocytes suggest a mechanism by which Cdc42 and Rac1 control INF2 that, in turn, regulates the formation of MAL-positive vesicles that transport Lck to the plasma membrane. In addition to their own importance, our findings could be useful for investigating the role of MAL in hematologic malignancies.[14-18]

Acknowledgments

We thank A. Jiménez and J. A. Rodríguez for technical assistance and Drs I. Correas, J. Millán, and F. Martín-Belmonte for their helpful comments. The expert technical advice of the personnel of the Optical and Confocal Microscopy and Flow Cytometry Units is gratefully acknowledged.

This work was supported by grants (BFU2009-07886 and CONSOLIDER COAT CSD2009-00016) to M.A.A. from the Ministerio de Ciencia e Innovación (MICINN), Spain.

Authorship

Contribution: M.A.A. designed experiments and wrote the paper; J.A.B. carried out the yeast 2-hybrid analysis; and L.A.-D., O.M.A., and R.M. performed the rest of the experiments.

Conflict-of-interest disclosure: The authors declare no competing financial interests.

Correspondence: Miguel A. Alonso. Centro de Biología Molecular "Severo Ochoa," CSIC-UAM, c/ Nicolás Cabrera 1, Universidad Autónoma de Madrid, Cantoblanco, 28049 Madrid, Spain; e-mail: maalonso@cbm.uam.es.

References

1. Lin J, Weiss A. T cell receptor signalling. *J Cell Sci.* 2001;114(2):243-244.
2. Fooksman DR, Vardhana S, Vasiliver-Shamis G, et al. Functional anatomy of T cell activation and synapse formation. *Annu Rev Immunol.* 2010; 28(1):79-105.
3. Ley SC, Marsh M, Bebbington CR, Proudfoot K, Jordan P. Distinct intracellular localization of Lck and Fyn protein tyrosine kinases in human T lymphocytes. *J Cell Biol.* 1994;125(3):639-649.
4. Bijlmakers M-JJE, Marsh M. Trafficking of an acylated cytosolic protein: newly synthesized p56lck travels to the plasma membrane via the exocytic pathway. *J Cell Biol.* 1999;145(3):457-468.
5. Shenoy-Scaria AM, Gauen LK, Kwong J, Shaw AS, Lublin DM. Palmitylation of an amino-terminal cysteine motif of protein tyrosine kinases p56lck and p59fyn mediates interaction with glycosyl-phosphatidylinositol-anchored proteins. *Mol Cell Biol.* 1993;13(10):6385-6392.
6. Kabouridis PS, Magee AI, Ley SC. S-acylation of LCK protein tyrosine kinase is essential for its signalling function in T lymphocytes. *EMBO J.* 1997;16(16):4983-4998.
7. Zimmermann L, Paster W, Weghuber J, Eckerstorfer P, Stockinger H, Schütz GJ. Direct observation and quantitative analysis of Lck-exchange between plasma membrane and cytosol in living T cells. *J Biol Chem.* 2010;285: 6063-6070.
8. Alonso MA, Millán J. The role of lipid rafts in signalling and membrane trafficking in T lymphocytes. *J Cell Sci.* 2001;114(22):3957-3965.
9. Millán J, Alonso MA. MAL, a novel integral membrane protein of human T lymphocytes, associates with glycosylphosphatidylinositol-anchored proteins and Src-like tyrosine kinases. *Eur J Immunol.* 1998;28(11):3675-3684.
10. Puertollano R, Martin-Belmonte F, Millan J, et al. The MAL proteolipid is necessary for normal apical transport and accurate sorting of the influenza virus hemagglutinin in Madin-Darby canine kidney cells. *J Cell Biol.* 1999;145(1):141-151.
11. Cheong KH, Zacchetti D, Schneeberger EE, Simons K. VIP17/MAL, a lipid raft-associated protein, is involved in apical transport in MDCK cells. *Proc Natl Acad Sci U S A.* 1999;96(11):6241-6248.
12. Martin-Belmonte F, Puertollano R, Millan J, Alonso MA. The MAL proteolipid is necessary for the overall apical delivery of membrane proteins in the polarized epithelial Madin-Darby canine kidney and Fischer rat thyroid cell lines. *Mol Biol Cell.* 2000;11(6):2033-2045.
13. Anton O, Batista A, Millan J, et al. An essential role for the MAL protein in targeting Lck to the plasma membrane of human T lymphocytes. *J Exp Med.* 2008;205(13):3201-3213.
14. Tracey L, Villuendas R, Ortiz P, et al. Identification of genes involved in resistance to interferon-α in cutaneous T-cell lymphoma. *Am J Pathol.* 2002;161(5):1825-1837.
15. Copie-Bergman C, Gaulard P, Maouche-Chretien L, et al. The MAL gene is expressed in primary mediastinal large B-cell lymphoma. *Blood.* 1999; 94(10):3567-3575.
16. Copie-Bergman C, Plonquet A, Alonso MA, et al. MAL expression in lymphoid cells: further evidence for MAL as a distinct molecular marker of primary mediastinal large B-cell lymphomas. *Mod Pathol.* 15(11):1172-1180.
17. Hsi ED, Sup SJ, Alemany C, et al. MAL is expressed in a subset of Hodgkin lymphoma and identifies a population of patients with poor prognosis. *Am J Clin Pathol.* 2006;125(5):776-782.
18. Traverse-Glehen A, Pittaluga S, Gaulard P, et al. Mediastinal gray zone lymphoma: the missing link between classic Hodgkin's lymphoma and mediastinal large B-cell lymphoma. *Am J Surg Pathol.* 2005;29(11):1411-1421.
19. Goode BL, Eck MJ. Mechanism and function of formins in the control of actin assembly. *Annu Rev Biochem.* 2007;76(1):593.
20. Wallar BJ, Alberts AS. The formins: active scaffolds that remodel the cytoskeleton. *Trends Cell Biol.* 2003;13(8):435-446.
21. Ishizaki T, Morishima Y, Okamoto M, Furuyashiki T, Kato T, Narumiya S. Coordination of microtubules and the actin cytoskeleton by the Rho effector mDia1. *Nat Cell Biol.* 2001;3(1):8-14.
22. Bartolini F, Moseley JB, Schmoranzer J, Cassimeris L, Goode BL, Gundersen GG. The formin mDia2 stabilizes microtubules independently of its actin nucleation activity. *J Cell Biol.* 2008;181(3):523-536.
23. Ridley AJ. Rho GTPases and actin dynamics in membrane protrusions and vesicle trafficking. *Trends Cell Biol.* 2006;16(10):522-529.
24. Chhabra ES, Higgs HN. INF2 is a WASP homology 2 motif-containing formin that severs actin filaments and accelerates both polymerization and depolymerization. *J Biol Chem.* 2006; 281(36):26754-26767.
25. Madrid R, Aranda JF, Rodríguez-Fraticelli AE, et al. The formin INF2 regulates basolateral-to-apical transcytosis and lumen formation in association with Cdc42 and MAL2. *Dev Cell.* 2010;18814-827.
26. Byrne JA, Nourse CR, Basset P, Gunning P. Identification of homo- and heteromeric interactions between members of the breast carcinoma-associated D52 protein family using the yeast two-hybrid system. *Oncogene.* 1998;16873-882.
27. Wilson SHD, Bailey AM, Nourse CR, Mattei MG, Byrne JA. Identification of MAL2, a novel member of the MAL proteolipid family, through interactions with TPD52-like proteins in the yeast two-hybrid system. *Genomics.* 2001;7681-88.
28. Boutros R, Fanayan S, Shehata M, Byrne JA. The tumor protein D52 family: many pieces, many puzzles. *Biochem Biophys Res Commun.* 2004;325(4):1115-1121.
29. Kreitzer G, Marmorstein A, Okamoto P, Vallee R, Rodriguez-Boulan E. Kinesin and dynamin are required for post-Golgi transport of a plasma-membrane protein. *Nat Cell Biol.* 2000;2(2):125-127.
30. Xu H, Littman DR. A kinase-independent function of Lck in potentiating antigen-specific T cell activation. *Cell.* 1993;74(4):633-643.
31. Akhmanova A, Steinmetz MO. Tracking the ends: a dynamic protein network controls the fate of microtubule tips. *Nat Rev Mol Cell Biol.* 2008;9(4): 309-322.
32. Taunton J. Actin filament nucleation by endosomes, lysosomes and secretory vesicles. *Curr Opin Cell Biol.* 2001;13(1):85-91.
33. Ploubidou A, Way M. Viral transport and the cytoskeleton. *Curr Opin Cell Biol.* 2001;13(1):97-105.
34. Xu Y, Moseley JB, Sagot I, et al. Crystal structures of a formin homology-2 domain reveal a tethered dimer architecture. *Cell.* 2004;116(5): 711-723.
35. Formaggio E, Cantù C, Chiamulera C, Fumagalli GF. p75 neurotrophin receptor distribution and transport in cultured neurons. *Neurosci Res.* 2008;62(1):32-42.
36. Vicente-Manzanares M, Rey M, Perez-Martinez M, et al. The RhoA effector mDia is induced during T cell activation and regulates actin polymerization and cell migration in T lymphocytes. *J Immunol.* 2003;171(2):1023-1034.
37. Eisenmann KM, West RA, Hildebrand D, et al. T cell responses in mammalian diaphanous-related formin mDia1 knock-out mice. *J Biol Chem.* 2007; 282(34):25152-25158.
38. Sakata D, Taniguchi H, Yasuda S, et al. Impaired T lymphocyte trafficking in mice deficient in an

actin-nucleating protein, mDia1. *J Exp Med.* 2007;204(9):2031-2038.

39. Wallar BJ, DeWard AD, Resau JH, Alberts AS. RhoB and the mammalian Diaphanous-related formin mDia2 in endosome trafficking. *Exp Cell Res.* 2007;313(3):560-571.
40. Gasman S, Kalaidzidis Y, Zerial M. RhoD regulates endosome dynamics through diaphanous-related formin and src tyrosine kinase. *Nat Cell Biol.* 2003;5(3):195-204.
41. Fernandez-Borja M, Janssen L, Verwoerd D, Hordijk P, Neefjes J. RhoB regulates endosome transport by promoting actin assembly on endosomal membranes through Dia1. *J Cell Sci.* 2005; 118(12):2661-2670.
42. Sandilands E, Cans C, Fincham VJ, et al. RhoB and actin polymerization coordinate Src activation with endosome-mediated delivery to the membrane. *Dev Cell.* 2004;7(6):855-869.
43. Sandilands E, Frame MC. Endosomal trafficking of Src tyrosine kinase. *Trends Cell Biol.* 2008; 18(7):322-329.
44. Rose R, Weyand M, Lammers M, Ishizaki T, Ahmadian MR, Wittinghofer A. Structural and mechanistic insights into the interaction between Rho and mammalian Dia. *Nature.* 2005;435(7041): 513-518.
45. Gorska MM, Liang Q, Karim Z, Alam R. Uncoordinated 119 protein controls trafficking of Lck via the Rab11 endosome and is critical for immunological synapse formation. *J Immunol.* 2009; 183(3):1675-1684.
46. Lapierre LA, Kumar R, Hales CM, et al. Myosin Vb is associated with plasma membrane recycling systems. *Mol Biol Cell.* 2001;12(6):1843-1857.
47. Thoulouze MI, Sol-Foulon N, Blanchet F, Dautry-Varsat A, Schwartz O, Alcover A. Human immunodeficiency virus type-1infection impairs the formation of the immunological synapse. *Immunity.* 2006;24(5):547-561.
48. Haller C, Rauch S, Fackler OT. HIV-1 Nef employs two distinct mechanisms to modulate Lck subcellular localization and TCR induced actin remodeling. *PLoS ONE.* 2007;2(11):e1212.